

INELASTIC INTERACTION OF 3.5-BeV/c  $\pi^-$  MESONS WITH PROTONS

M. S. AĬNUTDINOV, S. M. ZOMBKOVSKIĬ, Ya. M. SELEKTOR, and V. N. SHULYACHENKO

Institute of Theoretical and Experimental Physics

Submitted to JETP editor February 19, 1964

J. Exptl. Theoret. Phys. (U.S.S.R.) 47, 100-106 (July, 1964)

Inelastic interactions of 3.5-BeV/c  $\pi^-$  mesons with protons were studied with a liquid hydrogen chamber of 25 cm diameter. The angular and momentum distributions of the secondary particles are presented. Two resonances have been observed for the  $\pi^- + p \rightarrow \pi^- + \pi^+ + n$  reaction: one with a mass  $\sim 750$  ( $\rho^0$  meson) and another with  $\sim 1250$  ( $f^0$  meson). Simultaneous production of a  $\rho^0$  meson and isobars with masses  $> 1300$  MeV is suggested.

Up to the present time a large amount of experimental information has been accumulated which indicates that statistical calculations cannot explain multiple production processes in  $\pi$ -p or p-p collisions. The spectra and angular distributions of secondary  $\pi$  mesons from 2-prong stars in  $\pi$ -p collisions result mainly from peripheral interactions<sup>[1]</sup>; in an appreciable number of events  $\rho$ - and  $f$ -resonances are formed. The final-state interaction also affects 4-prong stars, although to a smaller degree.

In the present work we have investigated the inelastic interaction of 3.5-BeV/c  $\pi^-$  mesons with hydrogen. The  $\pi^-$  beam of the synchrotron at the Institute of Theoretical and Experimental Physics was momentum-analyzed in a deflecting magnet, carefully collimated, and directed into a liquid hydrogen bubble chamber of 25 cm diameter situated in a magnetic field of 14 kG. Approximately 80 000 pictures were taken; the average number of particles was 10-15  $\pi^-$  mesons per chamber expansion. The stereophotographs were double-scanned. Selected events with a track length greater than 3 cm were analyzed with an automatic measuring machine. The average error in angle measurement was 0.7°; the error in momentum determination corresponded to the uncertainty in measurement of the curvature in the chamber, which was about  $50 \mu$  (for example, for 0.5 BeV/c  $\pi$  mesons traversing 10 cm in the chamber, the error in determining the momentum was  $\sim 4\%$ ).

The distribution of the events studied in number of prongs is as follows:

No. of prongs:	2	4	6	8
No. of stars:	8938	3940	139	2
Cross section, mb:	$19.9 \pm 0.3$	$8.0 \pm 0.2$	$0.17 \pm 0.03$	—

The absolute cross sections have been normalized to a total cross section of 28 mb<sup>[2]</sup>. Stars consisting only of neutral particles were not taken

into account in the normalization.

Special interest is presented by the 2-prong stars, i.e., the reactions

$$\pi^- + p \rightarrow \pi^- + \pi^0 + p + k\pi^0, \quad k = 0, 1, \dots, \quad (1)$$

$$\pi^- + p \rightarrow \pi^- + \pi^+ + n + k\pi^0, \quad k = 0, 1, \dots \quad (2)$$

In reaction (1) the  $\pi^-$  mesons have a high momentum in the laboratory system, and separation of events with  $k = 0$  by means of energy balance is difficult. However, the literature indicates that even at high primary  $\pi$ -meson energies (6 BeV) reaction (1) occurs with  $k = 0$  in 75-80% of the cases (see, e.g., the work of Bellini<sup>[3]</sup>). For reaction (2) we carried out a calculation of the missing mass  $M_M$  for the two charged  $\pi$  mesons (i.e., the effective mass of the system of the neutron and the  $\pi^0$  mesons) according to the formula

$$M_M = [(E_0 - E_1 - E_2)^2 - (p_0 - p_1 - p_2)^2]^{1/2},$$

where  $E_0$  and  $p_0$  are the energy and momentum of the primary  $\pi^-$  meson;  $E_1$ ,  $p_1$ , and  $E_2$ ,  $p_2$  are respectively the energy and momentum of the secondary charged  $\pi$  mesons. The accuracy with which  $M_M$  is determined is 80-150 MeV, depending on the energy interval. Thus, the reaction  $\pi^- + p \rightarrow \pi^- + \pi^+ + n$  in the limits of the experimental errors corresponds to the mass interval  $800 \leq M_M \leq 1100$  MeV.

Figure 1 shows the angular and momentum distributions of  $\pi^-$  mesons from reaction (1), in the c.m. system. Figure 2 shows the same distributions for  $\pi$  mesons from reaction (2) for  $800 \leq M_M \leq 1100$  MeV. Our attention is drawn to the fact that the  $\pi^-$  angular distribution from reaction (1) has a sharp peak in the forward direction. The  $\pi^-$  angular distribution from reaction (2) in the interval  $800 \leq M_M \leq 1100$  MeV also has a peak at small angles, although it is somewhat less pro-

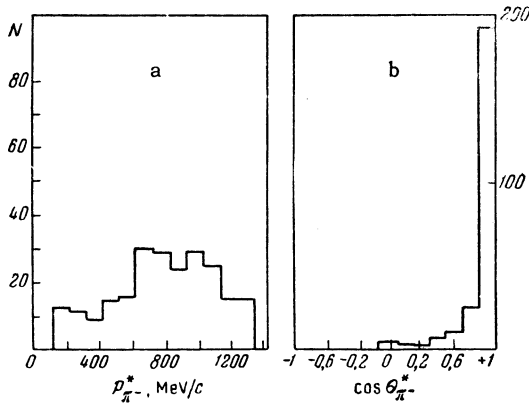


FIG. 1. Momentum and angular distributions (c.m.) of  $\pi^-$  mesons from reaction (1).

nounced than for reaction (1). Such a peak is completely absent in the  $\pi^+$  angular distribution.

The  $\pi^-$  momentum distribution from reaction (1) is appreciably different from the  $\pi^+$  distribution from reaction (2) for  $800 \leq M_m \leq 1100$  MeV. The  $\pi^-$  distribution from (1) is harder (more energetic), a noticeable fraction of the  $\pi^-$  mesons having a momentum close to that of elastically scattered  $\pi^-$  mesons. Similarly, the  $\pi^-$  spectrum from reaction (2) in the same interval of  $M_m$  is also harder than the  $\pi^+$  spectrum.

A possible mechanism leading to the appearance of a sharp peak in the  $\pi^-$  angular distribution from reaction (1) and a hard momentum spectrum of  $\pi^-$  mesons is diffraction scattering of the primary  $\pi^-$  meson by a virtual  $\pi$  meson in the one-meson diagram. The work of Bellini et al.<sup>[3]</sup> indicates that reaction (1) at higher  $\pi^-$  energies (6

and 18 BeV) occurs to a marked degree through diffraction scattering.

Another mechanism leading to the appearance of energetic  $\pi^-$  mesons at small angles in reaction (1) is the formation of "aligned"  $\rho^-$  mesons (the reaction  $\pi^- + p \rightarrow \rho^- + p$ ) with the subsequent decay  $\rho^- \rightarrow \pi^- + \pi^0$ . However, if events for which the effective mass of the  $\pi^- \pi^0$  system corresponds to the  $\rho$ -meson mass are excluded from the angular and momentum distributions for reaction (1), then the angular and momentum distributions for the remaining events turn out, as before, close to those shown in Fig. 1. Thus, the production and decay of  $\rho^-$  mesons cannot completely explain the  $\pi^-$  momentum and angular distributions from reaction (1).

To verify that one-meson exchange plays an important role in reaction (1) (mainly the reaction  $\pi^- + p \rightarrow \pi^- + \pi^0 + p$ ) and in reaction (2) for  $800 \leq M_m \leq 1100$  MeV (mainly the reaction  $\pi^- + p \rightarrow \pi^+ + \pi^- + n$ ), we made a Treiman-Yang plot<sup>[4]</sup>. For this purpose, we plotted in the center-of-mass system of the two secondary mesons ( $\pi^-$  and  $\pi^0$  mesons for reaction (1), and  $\pi^-$  and  $\pi^+$  mesons for reaction (2)) the distribution in the angle  $\varphi$  between the plane of the primary and secondary  $\pi^-$  meson directions and the plane formed by the directions of the nucleon before and after the collision. If an exchange occurs with one virtual  $\pi$  meson, correlation between these planes is absent and the angular distribution is isotropic. Thus, the existence of an isotropic distribution in a Treiman-Yang plot is a necessary (but, unfortu-

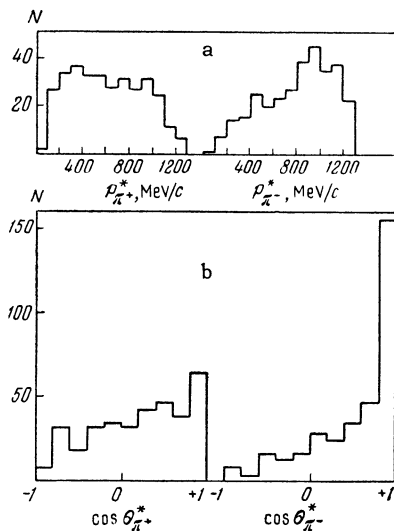


FIG. 2. Momentum and angular distributions (c.m.) of secondary  $\pi$ -mesons from reaction (2) for the interval  $800 \leq M_m \leq 1100$  MeV.

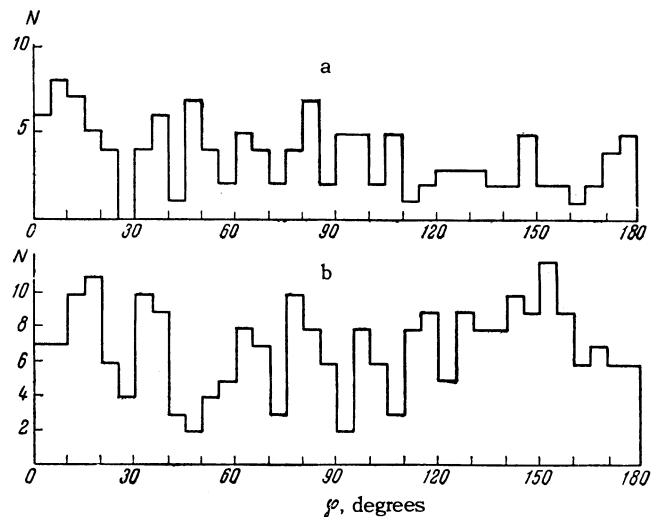


FIG. 3. Distribution in the angle between the plane formed by the primary and secondary  $\pi^-$  directions and the plane formed by the nucleon directions before and after the collisions: a) for reaction (1); b) for reaction (2) with  $800 \leq M_m \leq 1100$  MeV

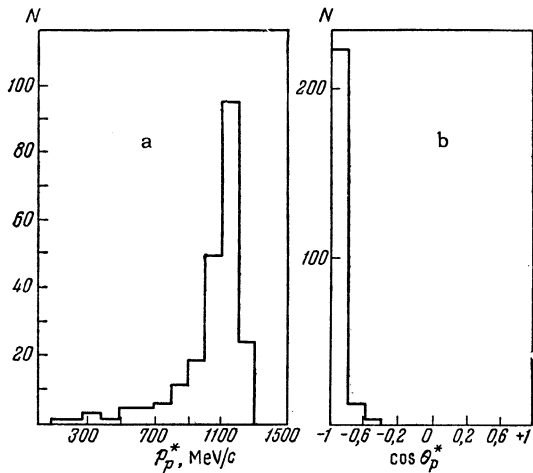


FIG. 4. C. m. proton distribution for reaction (1): a) momentum, b) angular.

nately, not sufficient) condition of one-meson exchange. Figure 3 shows the distribution obtained. Within the limits of the statistical errors, both distributions are isotropic, which argues in favor of one-meson exchange.

Figure 4 shows the angular and momentum distributions of the protons from reaction (1), in the c.m. system. It follows from Fig. 4 that the protons are emitted preferentially in the backward hemisphere. Figure 5 shows the momentum distribution of protons from reaction (1), in the laboratory system. Also shown in Fig. 5 are the

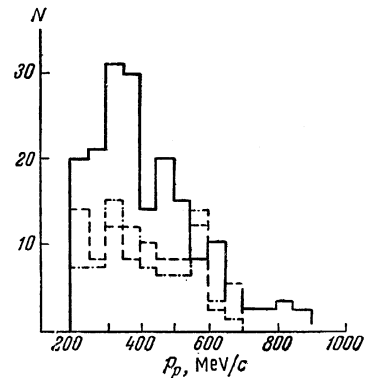


FIG. 5. The solid line is the momentum distribution (lab) of protons from reaction (1); the dashed line and the dot-dash line are from the paper of Bellini et al for 6 and 18 BeV, respectively.

momentum distributions for protons from reaction (1) for 6 and 18 BeV primary  $\pi^-$ -mesons, taken from the work of Bellini et al.<sup>[3]</sup> All three spectra are plotted for protons with momentum  $p \geq 200$  MeV/c. We conclude from Fig. 5 that no major increase in hardness of the proton spectra from reaction (1) is observed in the primary  $\pi^-$  momentum interval 3.5 to 18 BeV/c. (The average proton momenta in the region  $p \geq 200$  MeV/c for primary  $\pi^-$  momenta of 3.5, 6, and 18 BeV/c are respectively 420, 410, and 420 MeV/c.)

Figure 6, a shows the effective mass distribution of the  $\pi^+\pi^-$  system from reaction (2) for values of

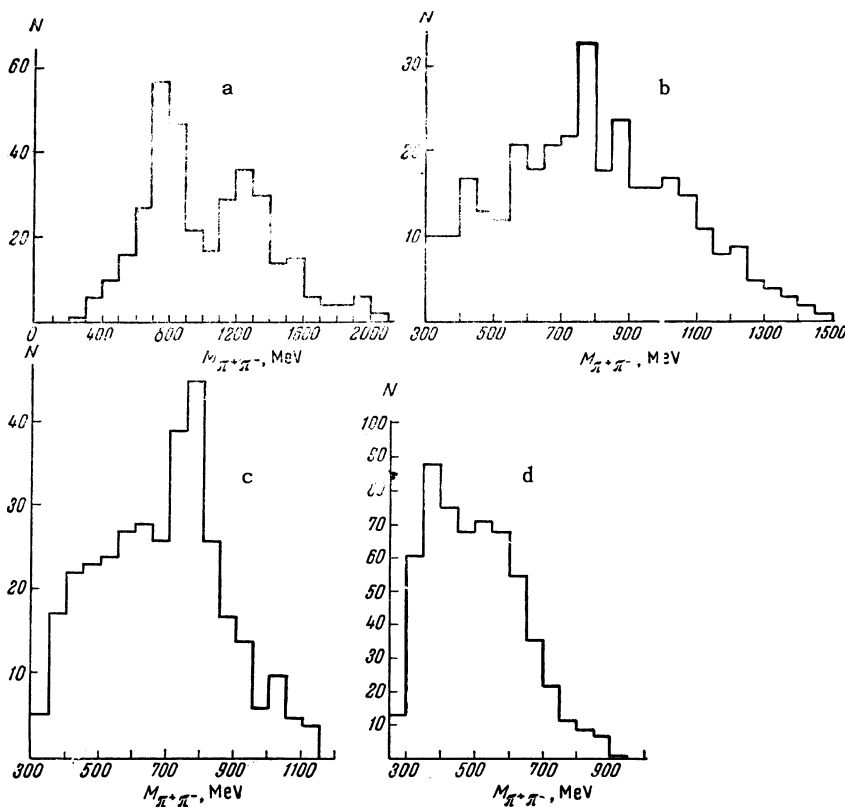
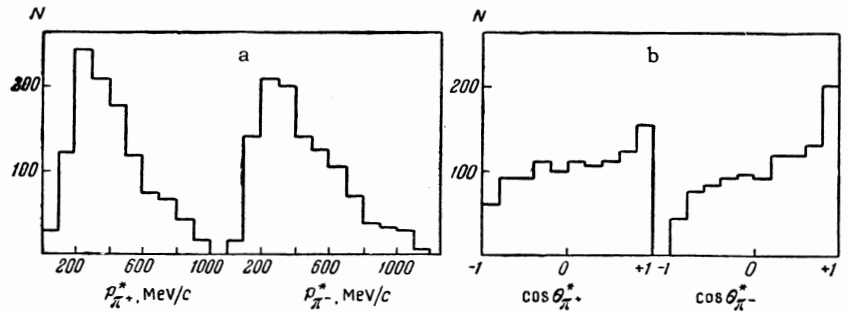


FIG. 6. Effective mass distributions of the  $\pi^+\pi^-$  system from reaction (2) for different intervals of  $\pi^+\pi^-$  system missing mass: a)  $800 \leq M_m \leq 1100$  MeV, 343 events; b)  $1100 \leq M_m \leq 1500$  MeV, 327 events; c)  $1500 \leq M_m \leq 1800$  MeV, 342 events; d)  $M_m \geq 1800$  MeV, 585 events.

FIG. 7. C. m. distributions of  $\pi$ -mesons from reaction (2) for  $M_m > 1100$  MeV: a) momentum, b) angular.



$M_m$  in the region 800-1100 MeV (i.e., for events predominantly from the reaction  $\pi^- + p \rightarrow \pi^- + \pi^+ + n$ ). The distribution distinctly shows two peaks corresponding to the formation of  $\rho^0$  and  $f^0$  mesons.

For  $M_m$  values in the interval 1100-1400 MeV (Fig. 6,b), i.e., in the interval which includes the  $3/2, 3/2$  isobar, the  $\rho^0$ -meson peak shows up only very weakly and, within the limits of error, cannot really be distinguished from the phase-space distribution. For the reaction  $\pi^+ + p \rightarrow \rho^0 + \pi^+ + p$  at a  $\pi^+$  energy of 2.90 BeV, Steinberger and his co-workers<sup>[5]</sup> have shown that the process occurs primarily through formation of the  $3/2, 3/2$  isobar. For the  $\pi^-$ -p interaction the reaction  $\pi^- + p \rightarrow \rho^0 + N_{3/2,3/2}$ , in agreement with charge independence, is suppressed by roughly a factor of four in comparison with the  $\pi^+$ -p interaction. The upper limit for the cross section for this reaction is consistent with the data recalculated from<sup>[5]</sup>.

In the interval  $1500 \leq M_m \leq 1800$  MeV (Fig. 6,c), a rather distinct peak corresponding to the  $\rho^0$ -meson mass is observed in the effective mass distribution for the  $\pi^+\pi^-$  system. In this range of  $M_m$  values, within the limits of resolution of our experiment, two isobars are found (at 1510 and 1680 MeV). The data obtained can be considered as an indication that the  $\rho^0$  meson can be produced not only with the isobar ( $3/2, 3/2$ ), but also with higher isobars.

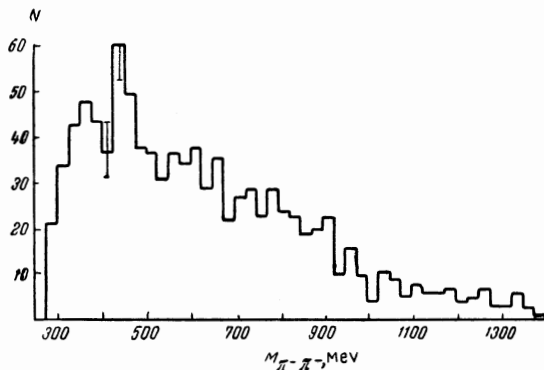


FIG. 8.  $\pi^+\pi^-$  effective mass distribution from 4-prong stars (980 combinations).

Figure 7 shows the center-of-mass momentum and angular distributions of  $\pi$  mesons for 2-prong stars from reaction (2) for  $M_m > 1100$  MeV. The table below lists the average momenta (c.m.) and the average transverse momenta (in MeV/c) of the  $\pi$  mesons:

	$\bar{p}^*(\pi^-)$	$\bar{p}^*(\pi^+)$	$\bar{p}_\perp(\pi^-)$	$\bar{p}_\perp(\pi^+)$
2-prong stars:	$500 \pm 15$	$450 \pm 15$	$325 \pm 50$	$345 \pm 35$
4-prong stars:	$380 \pm 15$	—	$360 \pm 40$	—

The transverse momenta are practically constant over the very wide primary momentum interval from 3 to 18 BeV/c (see, for example, Bellini et al.<sup>[3]</sup>).

In the course of this work we made calculations of the effective mass of all  $\pi$ -meson systems from many-prong stars. Figure 8 shows the effective mass distribution of two  $\pi$  mesons from 4-prong stars. Within the experimental error no resonant states are observed in the  $\pi^-\pi^-$  system ( $T = 2$ ).

We consider it our pleasant duty to express our gratitude to A. I. Alikhanov for numerous useful discussions. We are deeply grateful to the mathematical group headed by R. S. Guter for the calculations which they carried out, and also to the photographic analysis group headed by D. I. Tumanova and N. V. Vasil'eva.

<sup>1</sup>Selove, Hagopian, Brody, Baker, and Leboy, Phys. Rev. Letters 9, 272 (1962).

<sup>2</sup>von Dardel, Frisch, Mermod, Milburn, Piroué, Vivargent, Weber, and Winter, Phys. Rev. Letters 5, 333 (1960).

<sup>3</sup>Bellini, Fiorini, Herz, Negri, Ratti, Baglin, Bingham, Bloch, Drijard, Lagarrigue, Mittner, Orkin-Lecourtois, Rancon, Rousset, de Raad, Salmeron, and Voss, Nuovo cimento 27, 816 (1963).

<sup>4</sup>S. B. Treiman and C. Yang, Phys. Rev. Letters 8, 150 (1962).

<sup>5</sup>Alff, Berley, Colley, Gelfand, Nauenberg, Miller, Schultz, Steinberger, Tan, Brugger, Kramer, and Plano, Phys. Rev. Letters 9, 322 (1962).